Deep Learning-Based Magnetic Coupling Detection for Advanced Induction Heating Appliances

OSCAR LUCIA [1], **(Senior Member, IEEE), DENIS NAVARRO** [1],
PABLO GUILLÉN [1], **(Student Member, IEEE), HÉCTOR SARNAGO** [1], **(Senior Member, IEEE),
AND SERGIO LUCIA** [2], **(Member, IEEE)**
[1]Electronic Engineering and Communications Department, I3A, Universidad de Zaragoza, 50009 Zaragoza, Spain
[2]Einstein Center for Digital Future, Technische Universität Berlin, 10623 Berlin, Germany

Corresponding author: Oscar Lucia (olucia@unizar.es)

ABSTRACT Induction heating has become the reference technology for domestic heating applications due to its benefits in terms of performance, efficiency and safety, among others. In this context, recent design trends aim at providing highly flexible cooking surfaces composed of multi-coil structures. As in many other wireless power transfer systems, one of the main challenges to face is the proper detection of the magnetic coupling with the induction heating load in order to provide improved thermal performance and safe power electronic converter operation. This is specially challenging due to the high variability in the materials used in cookware as well as the random pot placement in flexible induction heating appliances. This paper proposes the use of deep learning techniques in order to provide accurate area overlap estimation regardless of the used pot and its position. An experimental test-bench composed of a complete power converter, multi-coil system and real-time measurement system has been implemented and used in this study to characterize the parameter variation with overlapped area. Convolutional neural networks are then proposed as an effective method to estimate the covered area, and several implementations are studied and compared according to their computational cost and accuracy. As a conclusion, the presented deep learning-based technique is proposed as an effective tool to estimate the magnetic coupling between the coil and the induction heating load in advanced induction heating appliances.

INDEX TERMS Inductive heating, resonant power conversion, wireless power transfer, deep learning, neural network, electromagnetic design, induction heating, home appliances.

I. INTRODUCTION

Induction heating (IH) [1] is a form of wireless power transfer which enables contactless heating of materials. It is based on applying an alternating magnetic field to the induction target or load (FIGURE 1), with frequencies which range usually from few kHz to several hundreds of kHz depending on the desired penetration depth and application. This magnetic field causes the heating of the material mainly by two physical phenomena: induced currents and magnetic hysteresis. In order to generate the required magnetic field,

The associate editor coordinating the review of this manuscript and approving it for publication was Zhixiang Zou.

power electronic converters are needed, being resonant power conversion commonly used due to its high efficiency and power density.

Induction heating offers the user many advantages derived from its inherent contactless nature. Since it is non-invasive heating method, it provides more reliable heating processes, safer and cleaner, being of great interest in industry. Besides, heating can be performed very quickly and with accurate control due to the use of high-performance power electronic converters, leading to superior heating systems. Last but not least, since the heating is directly performed in the induction heating load, efficiency is greatly improved compared with other heating methods due to the avoidance of thermal
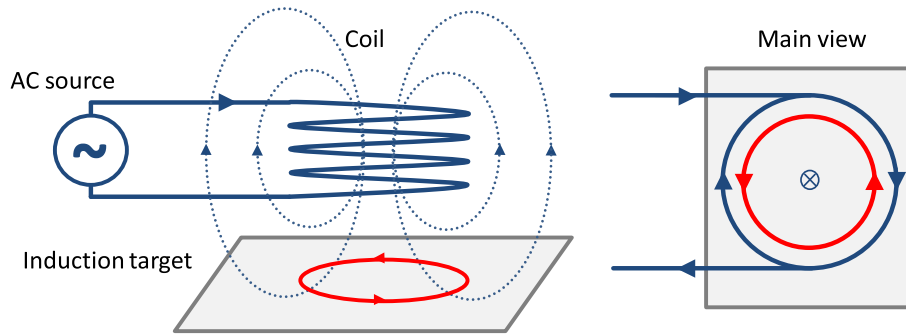
FIGURE 1. Induction heating fundamentals.

inertias and heat dissipated to the ambient. When specifically speaking of domestic induction heating [2], induction heating provides significant advantages compared with resistive or gas heating, including faster cooking, safer and cleaner operation, because the cooking surface reaches much lower temperatures, as well as more accurate control and improved efficiency. Because of these advantages, induction heating is nowadays being applied to a wide range of applications including, but not limited to, industrial [3], vehicular [4], domestic [5], and biomedical applications [6].

FIGURE 2. Domestic induction heating appliance.

A typical domestic induction heating appliance (FIGURE 2) is composed of the power electronic converter, the induction coil, a cooking surface, typically made of vitroceramic glass due to its excellent mechanical and aesthetical qualities, and the pan to be heated. The coil generates an alternating magnetic field that, in typical IH applications causes the heating of the target material by means of induced currents. In these conditions, the penetration depth δ is defined as:

$$\delta = \sqrt{\frac{\rho}{\pi \mu_0 \mu_r f}}, \tag{1}$$

where ρ and μ_r are the material resistivity and relative magnetic permeability, μ_0 is the vacuum magnetic permeability, and f is the excitation frequency generated by the inverter. These values change with the pot material and, consequently, so does the electrical equivalent seen by the inverter. The coupled induction coil – pan system is usually modelled as the series connection of an equivalent resistor and inductor, R_L, L_r, which forms part of a resonant tank that determines

the operation of the converter [2]. These equivalent electrical parameters are dependent of other parameters such as the pot materials, operating frequency, temperature and, specially, the coupling between the coil and the pan to be heated. For this reason, it is essential to obtain coupling information to optimize the induction heating system operation.

Despite the many advantages of domestic induction heating, there are still significant challenges to face. One of the most relevant is the magnetic coupling detection, which still remains unsolved for many wireless power transfer systems [7]. This is especially true when modern induction heating systems with multi-coil structures are being developed, where magnetic coupling has high variability and plays a key role in the converter performance. For this reason, the aim of this paper is to propose a deep learning-based magnetic coupling detection system. The prosed system will take advantage of a cost-effective and accurate measurement system for multi-coil architectures to extract the information required from the complete set of coils. Afterwards, convolutional neural networks (CNNs) will be used to estimate the percentage of area covered by the induction load in each coil. The proposed scheme has been developed using a 48-coil domestic induction heating prototype and several pan materials, proving the feasibility of this proposal.

The remaining of this paper is organized as follows. Section II introduces advances induction heating appliances, focusing on multi-coil structures, and provides a review of the state-of-the-art IH load identification techniques. Section III describes the proposed magnetic coupling detection system, including the power converter and measuring system, and the proposed neural network architecture and its training and data augmentation process. Finally, the results for different CNNs are presented and discussed in Section IV, and the main conclusions of this paper are summarized in Section V.

II. ADVANCED INDUCTION HEATING APPLIANCES
Nowadays, modern induction heating appliances have advanced towards providing higher user performance by adding improved power electronics for higher power, efficiency and power density, automatic cooking capabilities, temperature control, IoT and advanced interface capabilities, or integrated venting capabilities. One of the most successful research areas is the design of flexible cooking surfaces,
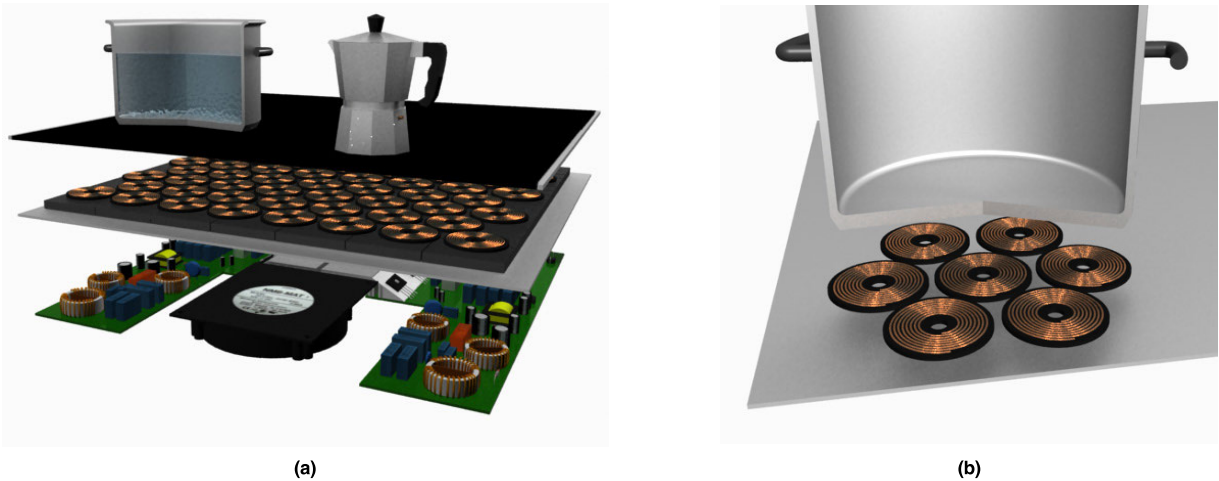
FIGURE 3. Advanced induction heating appliances: (a) total-active-surface concept and (b) detail of the coil-pot coupling.

also called total-active-surface concept, by using multi-coil arrays to implement a complete cooking surface [8]. This provides a superior user performance, since the user can use any pot, anywhere and with any shape, but at the same time implies new challenges for the power converter and magnetic coupling detection. This section reviews flexible cooking surfaces and the detection techniques previously proposed.

A. FLEXIBLE COOKING SURFACES

Flexible cooking surfaces are composed by a set of coils able to adapt its operation to the size, shape and position of the induction heating load/s. Initial implementations of such systems considered the use of concentric coils with different diameter that were activated depending on the size of the pot to be heated [9]. However, the pot center must be aligned with the inductor and, consequently, the position was still fixed.

Modern flexible induction heating appliances (FIGURE 3 (a)) are composed by a set of smaller coils [20], [21], typically more than 20, that can adapt to the size, shape and position of the induction heating loads. Consequently, the user obtains the highest flexibility degree in its use. In order to power such systems, typically specially

designed multiple-output resonant inverters are used. These include combinations of half/full-bridge structures [22], multi-inverter topologies [23], or matrix converters [24].

Despite the main advantages of flexible induction heating appliances, it is clear that in these configurations (FIGURE 3 (b)) the magnetic coupling is highly variable and, therefore, it is essential to provide a magnetic coupling detection system. This will allow not only to optimize the heating distribution, but also to provide safer operation of the inverter and those partly coupled coils. Next subsection reviews the previously proposed identification and detection systems.

B. REVIEW OF IDENTIFICATION AND DETECTION SYSTEMS

In the past, several identification and detection systems have been proposed in order to address and mitigate uncertainties inherent to the highly variable coupling in wireless power transfer systems and, more specifically, domestic induction heating systems. Table 1 summarizes the main proposed approaches in the state-of-the-art.

TABLE 1. Induction heating load identification and detection systems.

| Ref.	Year	IH Architecture	Measurement method	Identification principle	Output
[10]	2007	Single-inverter single-coil	Off-line scope	Optimization through dedicated power electronics identification HW	Equivalent electrical param.
[11]	2010	Single-inverter single-coil	Off-line scope	Correlation with FEM simulation	Magnetic properties
[12]	2012	Single-inverter single-coil	On-line coil oscillator	Frequency variation	Pot temperature
[13]	2014	Single-inverter single-coil	IR thermometry	Direct measurement	Pot temperature
[14]	2014	Single-inverter single-coil	Off-line scope	Particle Swarm Optimization	Equivalent electrical param.
[15]	2015	Multi-coil industrial	Off-line scope (On-line proposed)	Pseudo energy method	Equivalent electrical param.
[16]	2016	Multi-coil domestic system	Off-line impedance measurement	Impedance variation	Covered area
[17]	2018	Multi-coil domestic system	On-line voltage	DFT	Equivalent electrical param.
[18]	2018	Single-inverter single-coil	On-line voltage	Analytical expression evaluation	Equivalent electrical param.
[19]	2018	Single-inverter single-coil	On-line voltage / current	Neural network	Pot material
Proposed		Multi-coil domestic system	On-line voltage	Convolutional neural network	Covered area
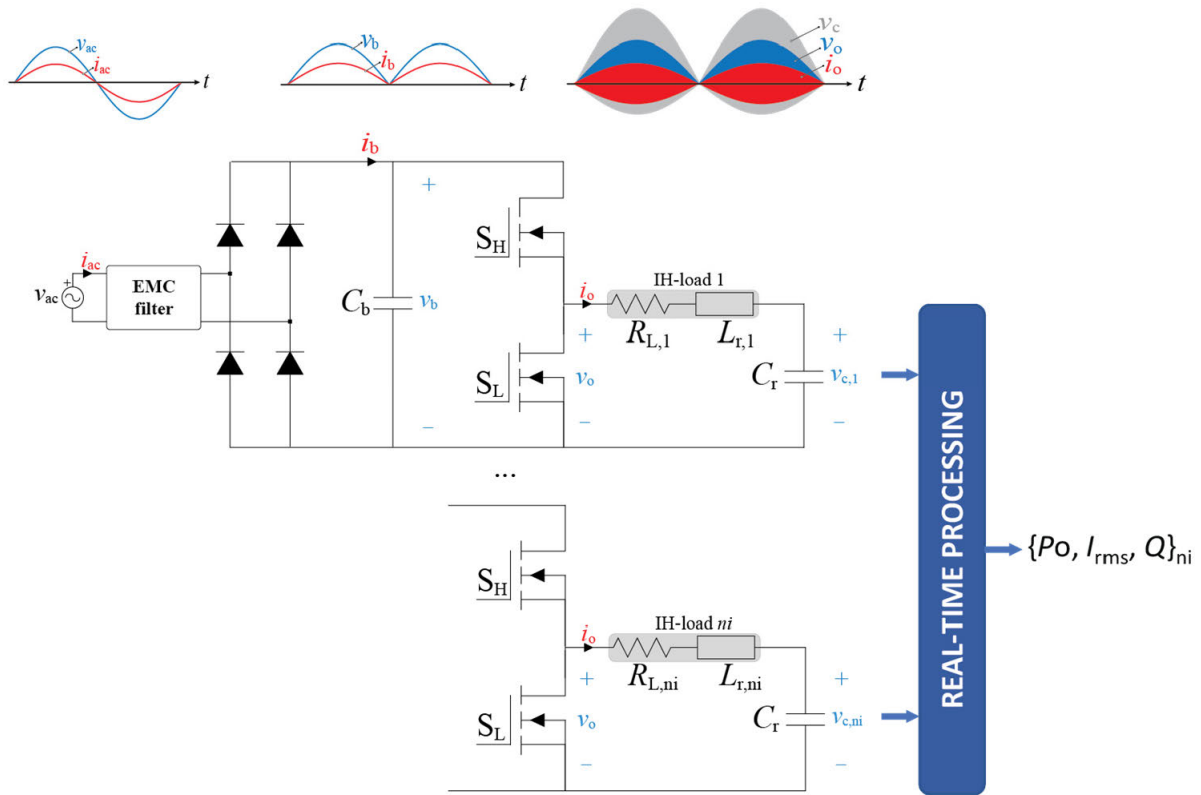
FIGURE 4. Power electronics and measurement architecture of the proposed system. The input current i_{ac} passes an electromagnetic compatibility filter (EMC) and its is rectified to obtain a dc- bus, i_b, v_b. After that, the inverters composed of S_H and S_L switches generates the medium frequency current to supply the resonant tank, i_o, composed of the coil-pot electrical equivalent, $R_{L,ni} - L_{r,ni}$, and the resonant capacitor C_r.

Most of the previously proposed techniques are aimed at obtaining the equivalent electrical parameters of the load. In [10], a high-performance hardware is proposed for on-line identification, whereas in [14] and [15] particle swarm optimization and the pseudo energy method are employed, respectively, to achieve off-line identifications. However, all these methods are only valid for off-line calculation. Only in [18] and [17], on-line identification of the equivalent electrical parameters is performed in real-time by evaluating simplified analytical expressions or DFT analysis, respectively.

Instead of focusing on the electrical parameters, other researches have studied IH load temperature to improve the heating process either using infrared sensors [13] or the IH coil as an inductive sensor [12]. In [11], off-line FEM simulations are correlated with experimental measurements to obtain the material magnetic properties. In [19], a neural network-based system was used to perform the classification of the pot material for a fixed single-inductor structure. Only in [16], off-line impedance variation is used to obtain an estimation of the covered area. However, this approach is not intended to be used in on-line identification or multi-load systems.

In this context, the aim of this paper is to provide a covered area estimation system based on convolutional neural networks that can provide an accurate estimation in modern multi-coil systems. Next section details the proposed system.

III. PROPOSED MAGNETIC COUPLING DETECTION SYSTEM

The proposed magnetic coupling detection system is based on using the information provided by the array of induction heating coils and processing it using a convolutional neural network. This section details the proposed power converter and measurement system, as well as the CNN structure and training procedure.

A. POWER ELECTRONICS AND MEASUREMENT ARCHITECTURE

In order to supply the proposed multi-coil architecture, a multiple output converter structure is proposed. FIGURE 4 shows the proposed power converter and measurement system for a *ni* IH loads system. It is based on a set of series resonant half-bridge inverters [25]. Each induction heating load is modelled by its equivalent electrical parameters, $R_{L,ni} - L_{r,ni}$. These elements form parts of the resonant power converter resonant tank, together with the resonant capacitor C_r, which is equal for all the inductors, and therefore significantly affects to the operation and the performance of each converter. It should be noted that the electrical equivalent parameters of each load change significantly with the IH load coupling and, therefore, it is essential to obtain this information to provide efficient and safe operation.

The equation that defines the operation for each load of the aforementioned circuit is:

$$R_L i_o(t) + L_r \frac{\mathrm{d}i_o(t)}{\mathrm{d}t} + \frac{1}{C_r} \int i_o(t)dt = v_o(t), \qquad (2)$$

In order to monitor the main operational parameters of the proposed multi-coil system, the resonant capacitor voltage is measured to provide an accurate and cost-effective estimation of parameters such as output power, P, output current, I_{rms}, quality factor, defined as $Q_i = \omega L_{r,i}/R_{L,i}$, or the soft-switching conditions. In the proposed system, these parameters are calculated from the values of the resonant capacitor voltage V_c using the following expressions [17]:

$$I_{o,rms}^2 = \frac{C_r}{L_r} \left(V_{c,rms}^2 - \frac{V_s}{T_{sw}} \int_0^{DT_{sw}} v_c(t)dt \right), \qquad (3)$$

$$Q_{sw} = \frac{\omega_{sw} C_r \left(V_{c,rms}^2 - \frac{V_s}{T_{sw}} \int_0^{DT_{sw}} v_c(t)dt \right)}{P_o}, \qquad (4)$$

$$P_o = f_{sw} C_r V_s \left(v_c(t=0) - v_c(t=DT_{sw}) \right), \qquad (5)$$

where D and T_{sw} are the applied switching period and duty cycle.

This measurement system will allow not only to provide the target output power desired by the user, but also to use this information to estimate the IH load coupling using the proposed deep learning techniques as it is explained in next subsection.

B. PROPOSED CONVOLUTIONAL NEURAL NETWORK

Deep neural networks have evolved in recent years to be applied to solve a wide range of engineering problems. One of the main reasons for the success of deep neural networks in recent years is that they do not require very detailed feature engineering efforts as other data-based methods, being able to learn complex patterns from large amounts of data [26]. A standard (fully connected) neural network $\mathcal{N}$ is composed of different layers that perform a linear transformation of the input data followed by a nonlinear transformation and can be mathematically described as:

$$\mathcal{N}(x) = \alpha_{L+1} \circ \beta_L \circ \alpha_L \circ \ldots \circ \beta_1 \circ \alpha_1(x), \qquad (6)$$

where x is the input to the neural network, L is the number of layers, α is an affine transformation and β is a nonlinear function. The nonlinearity applied to the data is usually a hyperparameter that can be chosen, but recently the non-saturation function, often called Rectifier Linear Unit (ReLU) has been very successful to avoid common problems during the training of large networks and is defined as:

$$\mathrm{ReLU} : \beta(x) = \max\{0, x\}. \qquad (7)$$

The use of Convolutional Neural Networks (CNNs) has been also a key component for the solution of complex problems using machine learning [27], especially in the field of image recognition [28], big data [29], or human motion pattern recognition [30]. A convolutional neural network uses a filter or *kernel*, which is typically of much smaller size than the original data dimensions. The kernel averages the local properties in a structured data set, such as an image or, in this case, the data from each IH coil. The underlying assumption is that in images, or in the case of the multi-coil system considered in this work, the properties of a pixel, or a coil, are strongly correlated with the properties of the neighboring elements. This enables the use of convolutional networks that have a significantly lower number of parameters than fully connected networks, because only the elements in the kernel need to be learned. As a result, deeper networks that can learn higher level abstractions can be designed and successfully trained [26]. In addition to this, CNNs has a much lower coefficient number than their fully-connected counterparts. This is a key benefit in low-memory implementations, such as the ones based in microcontrollers for the proposed applications.

Regardless of the architecture chosen for a neural network, the training is always performed by solving a complex non-convex optimization problem in which a measure of accuracy between the output and the known labels is minimized. Very often, and also done in this paper, the mean squared error is used so that the training procedure consists in solving the following optimization problem

$$\min_{W,b} \frac{1}{N_s} \sum_{i=1}^{N_s} (y^{(i)} - \mathcal{N}(x^{(i)}))^2, \qquad (8)$$

where W and b are the weights and biases that describe the affine transformations of each layer of the neural network $\mathcal{N}$, N_s is the total number of training samples. For each data pair i, the known label that corresponds to each input $x^{(i)}$ is denoted by $y^{(i)}$.

In this paper, the proposed multi-coil system will be used as sensor for the IH load coupling, neglecting the need of additional sensors (FIGURE 5, left). A CNN is proposed to be used to predict the area coverage of each inductor of the multi-coil system (FIGURE 5, right) based on the following input data for each one of the coils: output power, P, current, I_{rms}, and quality factor, Q.

A multi-coil system with a total of $ni = 48$ coils is considered. The proposed neural network uses a total of n convolutional layers with kernels of dimensions (i, j, k) for each input magnitude (P, I_{rms}, Q). Before the ReLU activation function is evaluated, each kernel is applied p_l times within the convolutional layer l. Pooling layers are not used, as it is often done in image recognition, because the size of the input data is manageable and does not need to be reduced. The kernel is moved one inductor at a time for each convolutional layer, that is the stride is chosen equal to one, and the input data is augmented with zeros on the boundary of the multi-coil system so that the dimensions of the data remain the same after applying the convolutional layer (padding is chosen equal to one). This is a common technique to deal with the borders of images or other structured data. The loss function is chosen as the mean squared error between the measured area coverage and the area coverage predicted by the network.
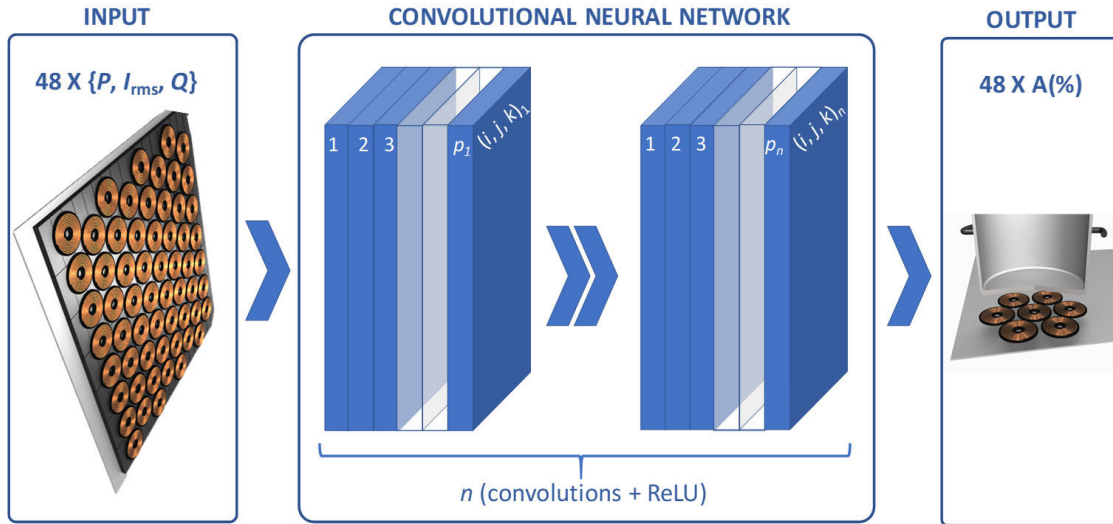
FIGURE 5. Proposed convolutional neural network-based area overlap estimation system. The input layer is 48 coils x 3 parameters whereas the output is the percentage of the area coverage in each of the 48 coils. Each convolution layer includes *p* kernels of dimensions *I, j, k* plus a ReLU layer.

C. TRAINING AND DATA AUGMENTATION

A major challenge for the successful application of machine learning in engineering applications is the need for large amounts of data that must be used within the training process. If the data needs to be collected experimentally, this can lead to very time and cost-intensive experiments that render the approach inapplicable in practice. This is especially important in the proposed multi-coil IH applications, since the number of combinations of pot diameters, materials and positions makes the problem unmanageable.

To mitigate this problem, in this work data augmentation techniques are used, which are also often used on other fields [31]–[33]. The experimental test-bench for data collection is shown in FIGURE 6(a), which is similar to a real 48-coil IH appliance. Considering that all coils are equal, the parameters of interest are experimentally obtained for different coverage areas in a single coil. Consequently, a set of pots of different materials and radius R are located above a coil of radius r, being $R \gg r$; and separated a distance d. Then, this distance d is modified to obtain the required parameters used as input of the CNN, i.e. P, I_{rms}, Q, for different area coverages. After this experimental data is available, data augmentation consists to expand this data to a full multi-coil system composed of ni elements (FIGURE 6(b)). Then, a set of pots of randomized radius R and materials are located in a random position, (c_x, c_y), over the multi-coil structure. After that, the covered area for each inductor is calculated using the following expression

$$
\begin{aligned}
A_{1\ldots ni} &= r^2 acos((d^2 + r^2 - R^2)/(2dr)) \\
&+ R^2 acos((d^2 + R^2 - r^2)/(2dR)) \\
&- 0.5\sqrt{(-d+r+R)(d+r-R)(d-r+R)(d+r+R)}.
\end{aligned}
\tag{9}
$$

(a)

(b)

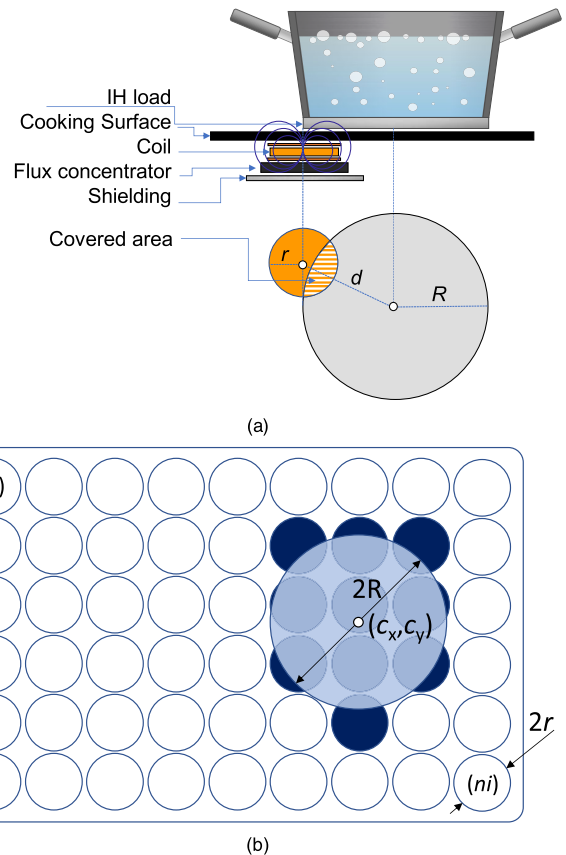**FIGURE 6.** Data augmentation scheme for NN training: (a) Detail of the structure under analysis and (b) complete system diagram.

Finally, the CNN input parameters for each coil, P, I_{rms}, Q, are obtained by linear interpolation of the experimental data. This technique has been applied to simulate the simultaneous presence of several pots over the cooking surface, enabling realistic operating conditions training. This

FIGURE 7. Experimental test-bench.

procedure enables the generation of large sets of data for training and test, based on experimental measurements, that are otherwise not feasible due to the large number of different combinations and required measurements.

IV. RESULTS

In order to test the proposed CNN-based magnetic coupling detection system, the experimental test-bench shown in FIGURE 7 has been used. It consists on a $ni = 48$ coil induction heating system supplied by a multiple-output resonant inverter with monitoring capabilities as shown in FIGURE 4.

TABLE 2. Equivalent electrical parameters of the studied materials.

Material	R_L	L_r	Q
Air	0.23 Ω	284 µH	>200
Aluminum	1.90 Ω	161 µH	26.33
Material #1	18,09 Ω	213 µH	3.70
Material #2	17.77 Ω	235 µH	4.16
Material #3	18.57 Ω	284 µH	4,81

To generate the required data, three different materials have been used, whose electrical parameters are summarized in Table 2. These materials present typical electrical values common in commercially available IH loads for the given coils. The radius of the coils is 4 cm and the radius of the pot is 12 cm. The procedure detailed in Section III is then applied to extract the experimental values of the electrical parameters, P, I_{rms}, Q, for different area coverages from 0 to 100% in 10% steps to properly account for the nonlinear behavior. FIGURE 8 summarizes the obtained values, which have been normalized to the value for 100% coverage, for the three different materials (#1-#3). An important conclusion is that the monitored parameters exhibit a non-linear and non-monotonous evolution, increasing the problem complexity and making CNN a suitable approach to build the proposed magnetic coupling detection system.

The previously detailed data augmentation technique is used to generate 10^6 data points for training the proposed convolutional networks and $2.5 \cdot 10^5$ data points for testing.
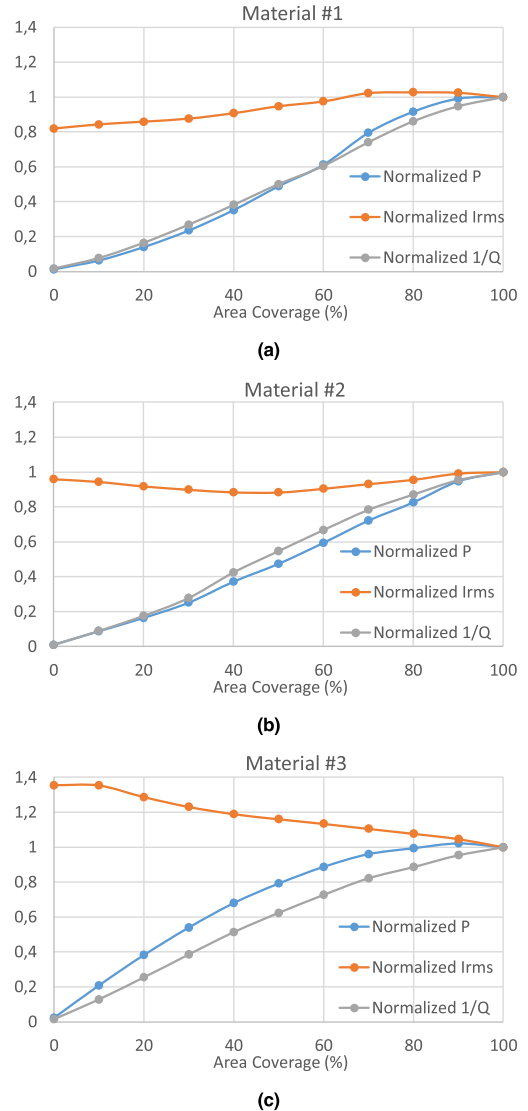

(a)

(b)

(c)

FIGURE 8. Evolution of the normalized parameters power (*P*), RMS current (*I*rms) and quality factor (*Q*) with the covered area for three different materials: material #1 (a), material #2 (b) and material #3 (c).

Since the final aim is the digital implementation of the proposed system, different CNN architectures have been studied and compared according to the required arithmetic resources and the obtained accuracy. Training has been performed using Caffe deep learning framework and the NVIDIA GTX1085Ti GPU. The training algorithm used is the adaptive moment estimation (ADAM), and the batch size used is 10^3.

Table 3 summarizes the studied convolutional neural network, considering its architecture, i.e. number of convolutions and kernel structure, and the obtained accuracy including root mean squared error (RMSE), maximum error (ME) and percentage of errors greater than 5%, expressed in area coverage %. Besides, multiply and accumulate blocks (MAC) have been considered as a relevant architecture index, since it is a direct indicator of the required digital hardware. The table also shows the number of coefficients that need to be stored

TABLE 3. Summary of studied convolutional neural network architectures.

#	MAC (# Coefficients)	# Conv	Kernels [p (i, j, k)]	RMSE	ME	E > 5%
1	54,000 (1125+21)	3	15 3x3x3 5 3x3x15 1 3x3x5	0.421	8.41	2.47e-05
2	150,000 (1875+21)	3	15 5x5x3 5 5x5x15 1 5x5x5	0.468	14.1	1.29e-04
3	234,576 (4644+40)	5	27 3x3x9 9 3x3x27 3 3x3x9 1 3x3x3	0. 327	6.96	3.85e-06
4	549,504 (11448+76)	6	9 3x3x3 27 3x3x9 27 3x3x27 9 3x3x27 3 3x3x9 1 3x3x3	0. 198	5.26	4.16e-08
5	651,600 (13575+49)	5	9 5x5x3 27 5x5x9 9 5x5x27 3 5x5x9 1 5x5x3	0.22	5.69	1.04e-07
6	2,124,144 (42795+157)	7	9 3x3x3 27 3x3x9 81 3x3x27 27 3x3x81 9 3x3x9 3 3x3x9 1 3x3x3	0. 141	4.33	0
7	4,958,496 (103302+238)	8	9 3x3x3 27 3x3x9 81 3x3x27 81 3x3x81 27 3x3x81 9 3x3x27 3 3x3x9 1 3x3x3	0.160	7.25	1.39e-06

The column headers span: "CNN Architecture" (MAC, # Conv, Kernels) and "CNN Results (% Area)" (RMSE, ME, E > 5%).

TABLE 4. Standard fully-connected implementations for comparison with the proposed CNN implementation.

#	MAC (# Coefficients)	# Hidden layers	Width	RMSE	ME	E > 5%
1	19,200 (19200+148)	1	100	1.3	35	1.6e-02
2	38,400 (38400+248)	1	200	1.1	26	9e-03
3	76,800 (76800+448)	1	400	1.1	27	8e-03
4	192,000 (192000 +1048)	1	1000	0.9	29	4e-03
5	29,200 (29200+248)	2	100	1.1	29	7e-3
6	78,400 (78400+448)	2	200	1.1	27	6e-3
7	236,800 (236800+848)	2	400	0.7	24	3e-3
8	39,200 (39200+348)	3	100	0.9	23	5e-3
9	118,400 (118400+648)	3	200	0.7	17	2e-3
10	396,800 (396800+1248)	3	400	0.6	24	1e-3
11	238,400 (238400+1248)	6	200	0.7	20	1.8e-3

The column headers span: "NN Architecture" (MAC, # Hidden layers, Width) and "NN Results (% Area)" (RMSE, ME, E > 5%).

to represent each neural network which is an indicator of the required memory. The number of coefficients is reported as the sum of two numbers which represent the coefficients needed to store the weights and the biases of each network. In this table, it can be seen that all the implementations achieve low RMSE and E>5% values. A critical parameter for this application is ME, since a significant error can lead to a coil/inverter overheating that may damage irreversibly the appliance. From this table, it can be seen that implementations number 3 and above achieve ME lower than 10%, being sufficient for the proposed applications.

Table 4 has been included for comparing the proposed CNN implementation with a standard fully-connected implementation. As it has been aforementioned, CNN benefits from the fact of having a structure that takes into account neighbor coils, providing much accurate results for a similar digital resources consumption. Moreover, fully-connected implementation requires to store a higher number of coefficients to represent the corresponding neural networks, which jeopardizes low-memory implementations typical of this application.

V. CONCLUSIONS

Flexible domestic induction heating appliances provide higher user performance by enabling a new total active surface concept. In this context, there is a high load variability and it is essential to provide new and effective magnetic coupling detection systems.

This paper has proposed a new magnetic coupling detection system for multi-coil architectures based on deep learning techniques taking advantage of an accurate and cost-effective measurement system. Due to the nature of the data, similar to problems in image recognition, convolutional neural networks are applied to obtain an accurate estimation of the covered area in each inductor.

In order to train the proposed neural network and test the proposed approach, a 48-load induction heating prototype has been used. Several neural network architectures have been studied and compared considering computational resources and accuracy. As a conclusion, the proposed magnetic coupling detection system achieves excellent accuracy for the domestic application, and it is proposed as an effective method to improve flexible induction heating appliances.

REFERENCES

[1] Ó. Lucía, P. Maussion, E. J. Dede, and J. M. Burdío, "Induction heating technology and its applications: Past developments, current technology, and future challenges," *IEEE Trans. Ind. Electron.*, vol. 61, no. 5, pp. 2509–2520, May 2014.

[2] O. Lucia, J. M. Burdio, I. Millan, J. Acero, and D. Puyal, "Load-adaptive control algorithm of half-bridge series resonant inverter for domestic induction heating," *IEEE Trans. Ind. Electron.*, vol. 56, no. 8, pp. 3106–3116, Aug. 2009.

[3] C. Li, Y. Zhou, P. Wang, X. Wang, S. Dong, J. Du, Z. Liao, C. Yao, J. Tan, and Y. Mi, "Design and experiments of electromagnetic heating forming technology," *IEEE Access*, vol. 7, pp. 62646–62656, 2019.

[4] S.-H. Yu, D.-J. Park, and K.-C. Kim, "Heat source analysis of an induction heater for an electric vehicle," *IEEE Trans. Magn.*, vol. 53, no. 6, Jun. 2017, Art. no. 8001104.

[5] O. Lucia, I. Cvetkovic, H. Sarnago, D. Boroyevich, P. Mattavelli, and F. C. Lee, "Design of home appliances for a DC-based nanogrid system: An induction range study case," *IEEE J. Emerg. Sel. Topics Power Electron.*, vol. 1, no. 4, pp. 315–326, Dec. 2013.

[6] F. Aki, T. Loi, H. Saito, and K. Mitobe, "Examination of the influence on precision of the wireless temperature measurement induction heating system by 37°C constant temperature environment," *IEEE Trans. Magn.*, vol. 54, no. 6, Jun. 2018, Art. no. 2800303.

[7] L. Xiang, Z. Zhu, J. Tian, and Y. Tian, "Foreign object detection in a wireless power transfer system using symmetrical coil sets," *IEEE Access*, vol. 7, pp. 44622–44631, 2019.

[8] O. Lucía, J. Acero, C. Carretero, and J. M. Burdío, "Induction heating appliances: Toward more flexible cooking surfaces," *IEEE Ind. Electron. Mag.*, vol. 7, no. 3, pp. 35–47, Sep. 2013.

[9] J. Acero, C. Carretero, I. Millán, Ó. Lucía, R. Alonso, and J. M. Burdí, "Analysis and modeling of planar concentric windings forming adaptable-diameter burners for induction heating appliances," *IEEE Trans. Power Electron.*, vol. 26, no. 5, pp. 1546–1558, May 2011.

[10] D. Puyal, C. Bemal, J. M. Burdío, I. Millán, and J. Acero, "Dual 1.5-MHz 3.5-kW versatile half-bridge series-resonant inverter module for inductive load characterization," in *Proc. 22nd Annu. IEEE Appl. Power Electron. Conf. Expo.*, Feb./Mar. 2007, pp. 1133–1139.

[11] J. Acero, O. Lucia, I. Millan, L. A. Barragan, J.-M. Burdio, and R. Alonso, "Identification of the material properties used in domestic induction heating appliances for system-level simulation and design purposes," in *Proc. 25th Annu. IEEE Appl. Power Electron. Conf. Expo. (APEC)*, Feb. 2010, pp. 439–443.

[12] C. Franco, J. Acero, R. Alonso, C. Sagues, and D. Paesa, "Inductive sensor for temperature measurement in induction heating applications," *IEEE Sensors J.*, vol. 12, no. 5, pp. 996–1003, May 2012.

[13] J. Lasobras, R. Alonso, C. Carretero, E. Carretero, and E. Imaz, "Infrared sensor-based temperature control for domestic induction cooktops," *Sensors*, vol. 14, no. 3, pp. 5278–5295, 2019.

[14] A. Dominguez, A. Otin, I. Urriza, L. A. Barragan, D. Navarro, and J. I. Artigas, "Load identification of domestic induction heating based on particle swarm optimization," in *Proc. IEEE 15th Workshop Control Modeling Power Electron. (COMPEL)*, Jun. 2014, pp. 1–6.

[15] B. A. Nguyen, Q. D. Phan, D. M. Nguyen, K. L. Nguyen, O. Durrieu, and P. Maussion, "Parameter identification method for a three-phase induction heating system," *IEEE Trans. Ind. Appl.*, vol. 51, no. 6, pp. 4853–4860, Nov./Dec. 2015.

[16] V. T. Kilic, E. Unal, and H. V. Demir, "Wireless metal detection and surface coverage sensing for all-surface induction heating," *Sensors*, vol. 16, no. 3, p. 363, 2016.

[17] H. Sarnago, Ó. Lucía, and J. M. Burdío, "FPGA-based resonant load identification technique for flexible induction heating appliances," *IEEE Trans. Ind. Electron.*, vol. 65, no. 12, pp. 9421–9428, Dec. 2018.

[18] H. Sarnago, O. Lucía, and J. M. Burdio, "A versatile resonant tank identification methodology for induction heating systems," *IEEE Trans. Power Electron.*, vol. 33, no. 3, pp. 1897–1901, Mar. 2018.

[19] A. Bono-Nuez, B. Martin-del-Brio, C. Bernal-Ruiz, F. J. Perez-Cebolla, A. Martinez-Iturbe, and I. Sanz-Gorrachategui, "The inductor as a smart sensor for material identification in domestic induction cooking," *IEEE Sensors J.*, vol. 18, no. 6, pp. 2462–2470, Mar. 2018.

[20] J. Acero, C. Carretero, R. Alonso, Ó. Lucía, and J. M. Burdío, "Mutual impedance of small ring-type coils for multiwinding induction heating appliances," *IEEE Trans. Power Electron.*, vol. 28, no. 2, pp. 1025–1035, Feb. 2013.

[21] V. T. Kilic, E. Unal, N. Yilmaz, and H. V. Demir, "All-surface induction heating with high efficiency and space invariance enabled by arraying squircle coils in square lattice," *IEEE Trans. Consum. Electron.*, vol. 64, no. 3, pp. 339–347, Aug. 2018.

[22] H. Sarnago, O. Lucia, A. Mediano, and J. M. Burdio, "Design and implementation of a high-efficiency multiple-output resonant converter for induction heating applications featuring wide bandgap devices," *IEEE Trans. Power Electron.*, vol. 29, no. 5, pp. 2539–2549, May 2014.

[23] Ó. Lucía, J. M. Burdío, L. A. Barragán, J. Acero, I. Millán, "Series-resonant multiinverter for multiple induction heaters," *IEEE Trans. Power Electron.*, vol. 25, no. 11, pp. 2860–2868, Nov. 2010.

[24] H. Sarnago, J. M. Burdío, and Ó. Lucía, "High-performance and cost-effective ZCS matrix resonant inverter for total active surface induction heating appliances," *IEEE Trans. Power Electron.*, vol. 34, no. 1, pp. 117–125, Jan. 2019.

[25] H. Sarnago, Ó. Lucía, A. Mediano, and J. M. Burdío, "Analytical model of the half-bridge series resonant inverter for improved power conversion efficiency and performance," *IEEE Trans. Power Electron.*, vol. 30, no. 8, pp. 4128–4143, Aug. 2015.

[26] Y. LeCun, Y. Bengio, and G. Hinton, "Deep learning," *Nature*, vol. 521, no. 7553, p. 436, 2015.

[27] D. Silver, A. Huang, C. J. Maddison, A. Guez, L. Sifre, G. van den Driessche, J. Schrittwieser, I. Antonoglou, V. Panneershelvam, M. Lanctot, S. Dieleman, D. Grewe, J. Nham, N. Kalchbrenner, I. Sutskever, T. Lillicrap, M. Leach, K. Kavukcuoglu, T. Graepel, and D. Hassabis, "Mastering the game of go with deep neural networks and tree search," *Nature*, vol. 529, no. 7587, p. 484, 2016.

[28] J. Ker, L. Wang, J. Rao, and T. Lim, "Deep learning applications in medical image analysis," *IEEE Access*, vol. 6, pp. 9375–9389, 2018.

[29] M. Chen, Y. Hao, K. Hwang, L. Wang, and L. Wang, "Disease prediction by machine learning over big data from healthcare communities," *IEEE Access*, vol. 5, pp. 8869–8879, 2017.

[30] N. Neverova, C. Wolf, G. Lacey, L. Fridman, D. Chandra, B. Barbello, and G. Taylor, "Learning human identity from motion patterns," *IEEE Access*, vol. 4, pp. 1810–1820, 2016.

[31] A. S. Razavian, H. Azizpour, J. Sullivan, and S. Carlsson, "CNN features off-the-shelf: An astounding baseline for recognition," in *Proc. IEEE Conf. Comput. Vis. Pattern Recognit. (CVPR) Workshops*, Jun. 2014, pp. 512–519.

[32] J. Salamon and J. P. Bello, "Deep convolutional neural networks and data augmentation for environmental sound classification," *IEEE Signal Process. Lett.*, vol. 24, no. 3, pp. 279–283, Mar. 2017.

[33] J. Ding, B. Chen, H. Liu, and M. Huang, "Convolutional neural network with data augmentation for SAR target recognition," *IEEE Geosci. Remote Sens. Lett.*, vol. 13, no. 3, pp. 364–368, Mar. 2016.

OSCAR LUCIA (S'04–M'11–SM'14) received the M.Sc. and Ph.D. degrees (Hons.) in electrical engineering from the Universidad de Zaragoza, Spain, in 2006 and 2010, respectively.

From 2006 to 2007, he held a research internship at the Bosch and Siemens Home Appliances Group. Since 2008, he has been with the Department of Electronic Engineering and Communications, Universidad de Zaragoza, where he is currently an Associate Professor. From 2009 to 2012, he was a Visiting Scholar with the Center of Power Electronics Systems (CPES), Virginia Tech. His main research interests include resonant power conversion, wide-bandgap devices, and digital control, mainly applied to contactless energy transfer, induction heating, electric vehicles, and biomedical applications. In these topics, he has published more than 70 international journal articles and 150 conference papers, and he has filed more than 35 patents.

Dr. Lucía is an Active Member of the Power Electronics (PELS) and Industrial Electronics (IES) Societies. He is a member of the Aragon Institute for Engineering Research (I3A). He is currently an Associate Editor of the IEEE Transactions on Industrial Electronics, the IEEE Transactions on Power Electronics, and IEEE Open Journal of the Industrial Electronics Society.

DENIS NAVARRO received the M.Sc. degree in microelectronics from the University of Montpellier, France, in 1987, and the Ph.D. degree from the University of Zaragoza, in 1992.

Since September 1988, he has been with the Department of Electronic Engineering and Communications, Universidad de Zaragoza, where he is currently a Professor. His current research interests include CAD for VLSI, low power ASIC design, and modulation techniques for power converters. He is involved in the implementation of new applications of integrated circuits. In 1993, he designed the first SPARC®microprocessor in Europe.

Dr. Navarro is a member of the Aragon Institute for Engineering Research (I3A).

PABLO GUILLÉN (S'19) received the M.Sc. degree in industrial engineering from the University of Zaragoza, Zaragoza, Spain, in 2017. He is currently pursuing the Ph.D. degree with the Department of Electronic Engineering and Communications, Universidad de Zaragoza. During 2017, he held a research internship with the Bosch and Siemens Home Appliances Group. His main research interests include resonant power converters and digital control applied to induction heating. He is a member of the Aragon Institute for Engineering Research (I3A).

HÉCTOR SARNAGO (S'09–M'15–SM'19) received the M.Sc. degree in electrical engineering and the Ph.D. degree in power electronics from the University of Zaragoza, Spain, in 2010 and 2013, respectively. He is currently a Senior Postdoctoral Researcher with the Department of Electronic Engineering and Communications, Universidad de Zaragoza, Spain. His main research interests include resonant converters and digital control for induction heating applications.

Dr. Sarnago is a member of the Aragon Institute for Engineering Research (I3A).

SERGIO LUCIA (M'16) received the M.Sc. degree in electrical engineering from the University of Zaragoza, in 2010, and the Dr.-Ing. degree in optimization and automatic control from TU Dortmund, in 2014. He then joined the Otto-von-Guericke Universität Magdeburg, and visited the Massachusetts Institute of Technology as a Post-doctoral Fellow.

Since May 2017, he has been an Assistant Professor with TU Berlin and holds the Chair Internet of Things for smart buildings with the Einstein Center Digital Future. His research efforts focus on decision-making under uncertainty, distributed control, and embedded optimization using micro-controllers and FPGAs in the framework of the Internet of Things. Applications of interest include smart buildings and Li-ion battery systems. Dr. Lucia is an active member of the IEEE CSS society. He is an Associate Editor of the *Journal of Process Control*.

• • •